Journal of Computer-Aided Molecular Design, 10 (1996) 535–544
ESCOM

J-CAMD 360

Tautomerism of xanthine and alloxanthine: A model for substrate recognition by xanthine oxidase

Begoña Hernández[a], Modesto Orozco[a,*] and Francisco J. Luque[b,*]

[a]*Department of Biochemistry and Molecular Biology, Faculty of Chemistry, University of Barcelona, Martí i Franquès 1, E-08028 Barcelona, Spain*
[b]*Department of Pharmacy, Section Physical Chemistry, Faculty of Pharmacy, University of Barcelona, Avinguda Diagonal s/n, E-08028 Barcelona, Spain*

Received 20 May 1996
Accepted 21 June 1996

Keywords: Xanthine; Xanthine oxidase; Tautomerism; Molecular recognition; Substrate binding

Summary

Tautomerism of neutral xanthine and alloxanthine has been examined both in the gas phase and in aqueous solution. The tautomeric preference in the gas phase has been studied by means of semiempirical and ab initio quantum-mechanical computations with inclusion of correlation effects at the Møller–Plesset level, and from density-functional calculations. The influence of solvent on the relative stability between tautomers has been estimated from self-consistent reaction field calculations performed with different models. The results provide a detailed picture of tautomerism for these biologically relevant purine bases. The functional implications in the recognition by xanthine oxidase are analyzed from inspection of the interaction patterns of the most stable tautomeric forms. A model for the recognition of these purine derivatives in the enzyme binding site is discussed.

Introduction

Xanthine oxidase (xanthine:O_2 oxidoreductase; EC1.2.3.2) plays a key role in the degradation metabolism of purines [1]. In this catabolic route adenosine is deaminated by adenosine deaminase (EC3.5.4.4) yielding inosine, which is subsequently decomposed into the ribose and the purine base, hypoxanthine (1,7-dihydro-6*H*-purin-6-one). Xanthine oxidase catalyzes the oxidation at position 2 of hypoxanthine yielding xanthine (1,7-dihydro-6*H*-purin-2,6-dione), which is also an intermediate product in the degradation of guanine. Xanthine also acts as a substrate of xanthine oxidase and further oxidation at position 8 leads to the formation of uric acid, the final degradation product of purines in humans (see Fig. 1). Defects in the purine metabolism result in an increase in the level of uric acid and eventually lead to deposition of sodium hydrogen urate monohydrate crystals in joints. The disease associated with this phenomenon is known as gout and is clinically treated by the antihyperuricemic drug allopurinol [2] (pyrazolo[3,4-*d*]pyrimidin-6-one). Allopurinol, a compound closely related to hypoxanthine, is also a substrate of xanthine oxidase, which upon oxidation yields the product alloxanthine (pyrazolo[3,4-*d*]pyrimidin-2,6-one) (Fig. 2). The latter compound inactivates the enzyme by irreversible coordination to the reduced form of xanthine oxidase [3], thus inhibiting formation of uric acid. Treatment of gout with allopurinol leads to excretion of purines, mainly as hypoxanthine and xanthine.

Xanthine oxidase, and the related xanthine dehydrogenase (xanthine:nad$^+$oxidoreductase; EC1.2.1.37), comprise two equivalent and independent subunits [4]. Each subunit contains one atom of molybdenum, one molecule of flavin adenine dinucleotide and two distinct iron–sulphur clusters. The molybdenum atom seems to be coordinated to a dithiolene side chain of the pterin cofactor, which may serve to modulate the reactivity of the molybdenum center and/or its reduction potential [5]. A phosphoserine residue seems to exist in the active site, but its specific role is not yet established. The enzyme has two spatially separated substrate-binding sites for the reducing substrate (xanthine, hypoxanthine) and the oxidizing

*To whom correspondence should be addressed.

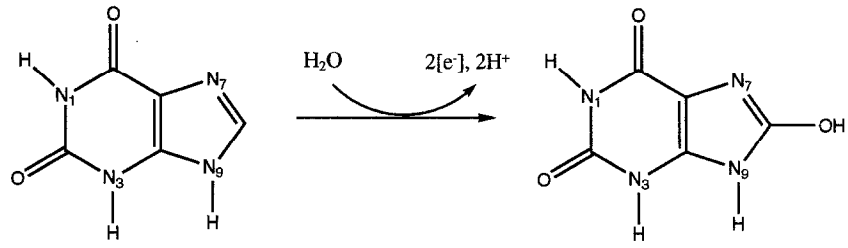

Xanthine Uric acid

Fig. 1. Representation of the enzymatic oxidation of xanthine catalyzed by xanthine oxidase.

substrate (O_2, NAD^+). The enzyme follows a two-site ping-pong mechanism [4,6], in which all the prosthetic groups participate in catalysis forming an electron-transport chain connecting the two binding sites.

Electron paramagnetic resonance, X-ray absorption spectroscopy and Raman spectra have been extensively used to identify the structural and kinetic aspects of the catalytic mechanism of xanthine oxidase [4]. The basic unit of the molybdenum center consists of a MoOS unit, the M=O moiety being common to each of the oxomolybdenum enzymes known to date [4c,d]. A rationale for the catalytic requirement of a sulfido group in xanthine oxidase is that the sulfur atom is involved in abstraction of the acidic proton attached to position C8 of xanthine. This step will trigger the catalytic reaction, which subsequently consists of carbanion attack on the oxygen of the Mo=O unit. Experimental studies suggest that the catalytically labile oxygen incorporated into xanthine is most likely that of the Mo=O unit, which is regenerated from the solvent water molecules in the course of each catalytic cycle.

Despite these findings, there is no detailed information about the interactions involved in recognition and binding of substrates. Knowledge of the molecular determinants that modulate substrate recognition is valuable in the design of inhibitors of xanthine oxidase [3,7]. For instance, purine-like inhibitors can interfere in other routes of purine metabolism [8], and information about the recognition pattern would be useful for designing specific inhibitors lacking undesirable side effects. We have recently examined the functional implications of the tautomerism of hypoxanthine and allopurinol in substrate recognition [9] by xanthine oxidase. Since each tautomer has a specific pattern of hydrogen-bond donors and acceptors, which presumably modulate anchoring to the enzyme active site, inspection of the tautomeric preference allowed us to discuss the recognition of these compounds by xanthine oxidase. In the present study our aim is to analyze the suitability of such a scheme of interactions between the substrate and the enzyme binding site to the recognition of xanthine and alloxanthine.

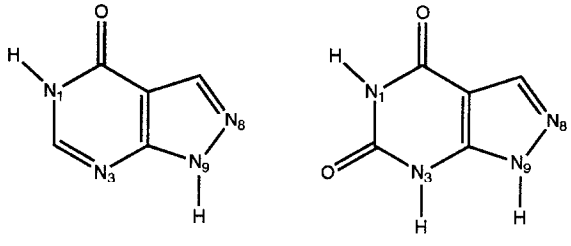

Allopurinol Alloxanthine

Fig. 2. Chemical structure of allopurinol and alloxanthine.

Xanthine and alloxanthine are closely related structures, which differ in the nature of the five-membered ring (imidazole versus pyrazole). These compounds can exist as a mixture of different tautomers resulting from lactam–lactim equilibria and from prototropic tautomerism at the imidazole and pyrazole moieties. In this study we have examined the tautomerism of xanthine and alloxanthine in the gas phase and in aqueous solution. Ab initio quantum-mechanical (QM) methods at the self-consistent field (SCF) and Møller–Plesset levels and density-functional theory (DFT) calculations are used to explore the tautomeric preference in the gas phase. The solvent effect is introduced by means of self-consistent reaction field (SCRF) continuum methods. The scheme of potential interactions that determines substrate recognition is discussed based on the relative stabilities between tautomers. Comparison of such a scheme with that reported for hypoxanthine and allopurinol [9] allows us to define a model for purine recognition by xanthine oxidase.

Methods

Owing to the large number of possible tautomers of xanthine and alloxanthine, and the large cost of ab initio QM calculations, a stepwise elimination scheme was adopted to study all the tautomeric species of these compounds and to obtain accurate data on the most stable forms. In this way the relative stability of all the tautomers of these compounds was determined at a low level of QM theory, and only the most stable species were further analyzed at the highest level. Thus, the relative stability in the gas phase was determined at the AM1 [10] semiempirical level, and the influence of hydration on the tautomerism was estimated from AM1-SCRF calculations (see below). Tautomers whose stability with respect to the

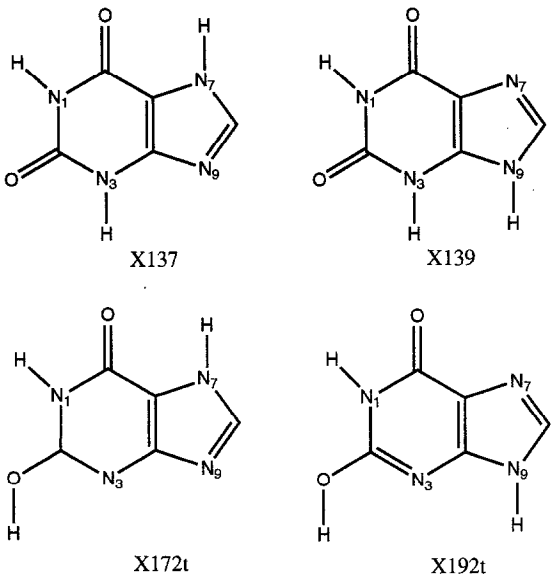

Fig. 3. Representation of the four tautomers of the neutral xanthine included in the final study after the stepwise elimination process (see text for details).

most stable species was less than 15 kcal/mol (either in the gas phase or in aqueous solution) were considered for further analysis at the ab initio level. Initially, a gas-phase geometry optimization at the HF/6-31G(d) [11] level was performed, and the solvent effect was estimated by means of ab initio 6-31G(d) SCRF calculations (see below). This allowed us to drastically limit the number of tautomers included in the final part of the study. Those tautomers whose free energy difference relative to the most stable species was less than 10 kcal/mol (either in the gas phase or in aqueous solution) were considered in the final part of the study.

In the final study single-point calculations at the SCF and second-order Møller–Plesset perturbation [12] (MP2) levels were carried out with the 6-31+G(d,p) basis [13]. In addition, DFT calculations were performed using the Becke3–Lee–Yang–Parr (B3LYP) functional [14]. The HF/6-31G(d) optimized geometry was used for all these calculations. Previous studies have shown that the refinement of structural parameters at higher computational levels has a very small effect on the tautomerism of closely related structures [15]. In all cases, thermal and entropic corrections were computed from the HF/6-31G(d) geometries using the standard procedure in GAUSSIAN '92-DFT [16].

The free energy of tautomerization in aqueous solution was determined according to Eq. 1. Relative free energies of hydration ($\Delta\Delta G^{aq}_{A\rightarrow B}$) were computed from the absolute free energies of hydration (ΔG^{hyd}_{A}, ΔG^{hyd}_{B}), as determined from SCRF calculations using the AM1 [17] and ab initio 6-31G(d) [18] optimized versions of the continuum model developed by Miertus, Scrocco and Tomasi (MST) [19]. The corresponding gas-phase optimized geometries were used in the calculations, since small geometrical effects are expected for rigid molecules like those considered here [9,20]. Nevertheless, in order to assess the relevance of solvent-induced geometrical changes for the stability between tautomers, AM1-SM2 calculations [21] were performed using the gas-phase AM1 geometry and by optimizing the geometry in aqueous solution:

TABLE 1
DIFFERENCES IN ENERGY, ENTHALPY AND FREE ENERGY IN THE GAS PHASE (RELATIVE TO THE TAUTOMER X137) FOR SELECTED TAUTOMERS OF XANTHINE DETERMINED AT VARIOUS COMPUTATIONAL LEVELS

Tautomer[a]	Method[b]	Energy differences (kcal/mol)		
		ΔE	ΔH	ΔG
X139	A	8.7	8.3	8.1
	B	9.0	8.7	8.5
	C	9.3	9.0	8.8
	D	9.2	8.9	8.7
X192t	A	14.3	14.1	14.4
	B	12.8	12.6	12.9
	C	11.4	11.2	11.5
	D	12.6	12.4	12.7
X172t	A	14.0	13.8	14.1
	B	12.0	11.8	12.1
	C	9.8	9.6	9.9
	D	10.9	10.7	11.0

[a] The nomenclature for the tautomers is given in Fig. 3.
[b] Method A: HF/6-31G(d)//HF/6-31G(d).
Method B: HF/6-31+G(d,p)//HF/6-31G(d).
Method C: MP2/6-31+G(d,p)//HF/6-31G(d).
Method D: B3LYP(6-31+G(d,p))//HF/6-31G(d).

TABLE 2
DIFFERENCES IN ENERGY, ENTHALPY AND FREE ENERGY IN THE GAS PHASE (RELATIVE TO THE TAUTOMER AX138) FOR SELECTED TAUTOMERS OF ALLOXANTHINE

Tautomer[a]	Method[b]	Energy differences (kcal/mol)		
		ΔE	ΔH	ΔG
Ax139	A	3.5	3.7	3.5
	B	3.8	4.0	3.8
	C	4.8	5.0	4.8
	D	4.2	4.4	4.2
Ax192t	A	10.7	10.8	11.0
	B	9.0	9.1	9.3
	C	8.4	8.5	8.7
	D	8.9	9.0	9.2
Ax182t	A	15.4	15.5	15.8
	B	13.4	13.5	13.8
	C	10.5	10.6	10.9
	D	11.9	12.0	12.3

[a] The nomenclature for the tautomers is given in Fig. 4.
[b] Method A: HF/6-31G(d)//HF/6-31G(d).
Method B: HF/6-31+G(d,p)//HF/6-31G(d).
Method C: MP2/6-31+G(d,p)//HF/6-31G(d).
Method D: B3LYP(6-31+G(d,p))//HF/6-31G(d).

$$\Delta G^{aq}_{A\to B} = \Delta G^{gas}_{A\to B} + \Delta G^{hyd}_{B} - \Delta G^{hyd}_{A} = \Delta G^{gas}_{A\to B} + \Delta\Delta G^{hyd}_{A\to B} \quad (1)$$

Patterns of interaction with potential electrophilic and nucleophilic groups were determined using the Molecular Interaction Potential (MIP) [22]. Standard optimized van der Waals parameters were used to describe the steric interactions of the quantum particle [22b]. In all cases, the wavefunctions determined from calculations in the gas phase at the SCF level with the 6-31G(d) basis in the evaluation of the MIP.

Calculations in the gas phase were carried out using the MOPAC93-Rel.A [23] and GAUSSIAN '92-DFT [16] computer programs. MST calculations were performed with locally modified versions of MOPAC93-Rel.A and MONSTERGAUSS [24]. AM1-SM2 calculations were performed using the AMSOL program [25] developed by Cramer and Truhlar. The MIP was computed using the MOPETE computer program [22c]. All the simulations were performed on the Cray-YMP of the Centre de Supercomputació de Catalunya, Spain, and on HP and SGI workstations in our laboratory.

Results

Tautomerism of xanthine and alloxanthine in the gas phase

Four tautomers of the neutral xanthine were considered after screening (detailed results of the screening in the stepwise elimination scheme are available upon request from the authors) in the stepwise elimination protocol (see Methods): two di-keto (X137 and X139) and two keto–enol (X192t and X172t) forms, which are shown in Fig. 3. All the di-enol tautomers were largely unstable and were not considered for further studies. Indeed, all the keto–enol tautomers with the hydroxyl group at position 6 were also greatly destabilized, which probably can be attributed to unfavorable repulsion between the lone pairs of the vicinal pyridine-like nitrogen (N1 or N3) and the carbonyl oxygen (>C2=O). This situation was also found for N3-H keto–enol tautomers having the hydroxyl group at position 2. Finally, the N1-H keto–enol species enolized at position 2 with the hydroxyl hydrogen oriented towards N1 were also excluded, most likely resulting from repulsion between hydrogens at N1-H and (>C2-OH) groups.

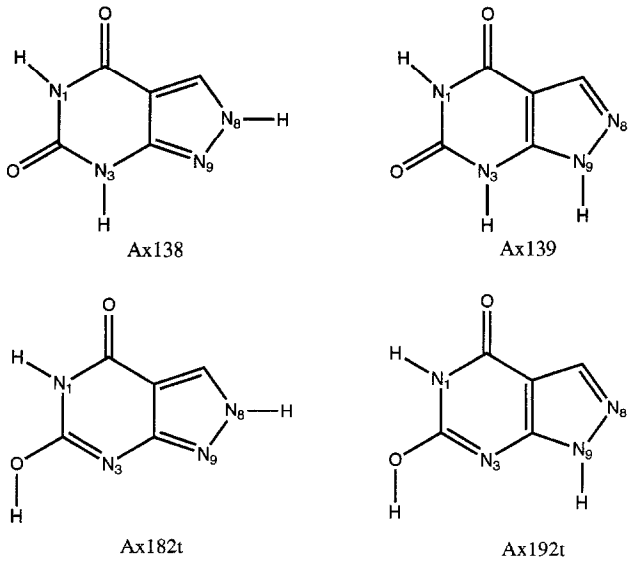

Fig. 4. Representation of the four tautomers of the neutral alloxanthine included in the final study after the stepwise elimination process (see text for details).

The relative stabilities estimated at the SCF, MP2 and DFT levels with the 6-31+G(d,p) basis for the selected tautomers are given in Table 1. All levels of computation clearly indicate that the keto tautomer X137 is the most stable in the gas phase. A large difference in stability is observed for the prototropic tautomerism between nitrogens N7 and N9 (the X139 species is about 8–9 kcal/mol less stable). Such a difference is even increased by at least 1 kcal/mol when the keto–enol tautomers X192t and X172t are considered.

Four tautomers of the neutral alloxanthine (see Fig. 4) were also selected according to the stepwise selection protocol: two di-keto (Ax138 and Ax139) and two keto–

TABLE 3
DIFFERENCES IN THE FREE ENERGY OF HYDRATION (RELATIVE TO THE TAUTOMER X137) OF SELECTED TAUTOMERS OF XANTHINE

Tautomer	Energy differences (kcal/mol)			
	$AMSOL^{AM1\text{-}SM2,g}$	$AMSOL^{AM1\text{-}SM2,s}$	MST^{AM1}	$MST^{6\text{-}31G(d)}$
X139	−1.9	−2.7	−5.2	−4.8
X192t	−1.8	−2.2	−2.0	−0.7
X172t	−1.3	−1.4	−1.8	0.3

$AMSOL^{AM1\text{-}SM2}$ calculations were performed with the geometry optimized in the gas phase ($AMSOL^{AM1\text{-}SM2,g}$) or with geometry optimization in solution ($AMSOL^{AM1\text{-}SM2,s}$). MST calculations were performed at the AM1 (MST^{AM1}) and 6-31G(d) ($MST^{6\text{-}31G(d)}$) levels using the corresponding gas-phase-optimized geometry.

TABLE 4
DIFFERENCES IN THE FREE ENERGIES OF HYDRATION (RELATIVE TO THE TAUTOMER AX138) OF SELECTED TAUTOMERS OF ALLOXANTHINE

Tautomer	Energy differences (kcal/mol)			
	$AMSOL^{AM1\text{-}SM2,g}$	$AMSOL^{AM1\text{-}SM2,s}$	MST^{AM1}	$MST^{6\text{-}31G(d)}$
Ax139	1.5	0.5	−0.9	−1.5
Ax192t	1.7	1.8	2.0	1.3
Ax182t	−1.1	−1.1	−1.2	−0.4

$AMSOL^{AM1\text{-}SM2}$ calculations were performed with the geometry optimized in the gas phase ($AMSOL^{AM1\text{-}SM2,g}$) or with geometry optimization in solution ($AMSOL^{AM1\text{-}SM2,s}$). MST calculations were performed at the AM1 (MST^{AM1}) and 6-31G(d) ($MST^{6\text{-}31G(d)}$) levels using the corresponding gas-phase-optimized geometry.

TABLE 5
FREE ENERGIES OF TAUTOMERIZATION ($\Delta G^{aq}_{A\to B}$, RELATIVE TO THE TAUTOMER X137) OF SELECTED TAUTOMERS OF XANTHINE

Tautomer	Energies (kcal/mol)		
	$\Delta G^{aq\text{-AMSOL}}_{A\to B}$	$\Delta G^{aq\text{-MST(AM1)}}_{A\to B}$	$\Delta G^{aq\text{-MST(6-31G(d))}}_{A\to B}$
X139	6.9	3.6	4.0
X192t	9.7	12.4	10.8
X172t	8.8	8.7	9.5

The values were estimated from the addition of the free energy of tautomerization in the gas phase at the MP2/6-31+G(d,p)) level to the free energy of hydration determined from AMSOL(AM1-SM2), MST(AM1) and MST(6-31G(d)) calculations (Eq. 1).

TABLE 6
FREE ENERGIES OF TAUTOMERIZATION ($\Delta G^{aq}_{A\to B}$; RELATIVE TO THE TAUTOMER AX138) OF SELECTED TAUTOMERS OF ALLOXANTHINE

Tautomer	Energies (kcal/mol)		
	$\Delta G^{aq\text{-AMSOL}}_{A\to B}$	$\Delta G^{aq\text{-MST(AM1)}}_{A\to B}$	$\Delta G^{aq\text{-MST(6-31G(d))}}_{A\to B}$
Ax139	6.3	3.9	3.3
Ax192t	10.4	10.7	5.6
Ax182t	9.8	9.7	9.4

The values were estimated from the addition of the free energy of tautomerization in the gas phase at the MP2/6-31+G(d,p)) level to the free energy of hydration determined from AMSOL(AM1-SM2), MST(AM1) and MST(6-31G(d)) calculations (Eq. 1).

enol (Ax192t and Ax182t) forms. Like for xanthine, all the di-enol tautomers, the keto–enol forms enolized at position 6 and the N3-H keto–enol species enolized at position 2 were largely unstable and were not considered further. The N1-H keto–enol forms with the hydroxyl hydrogen (>C2-OH) *cis* to N1 were not selected either.

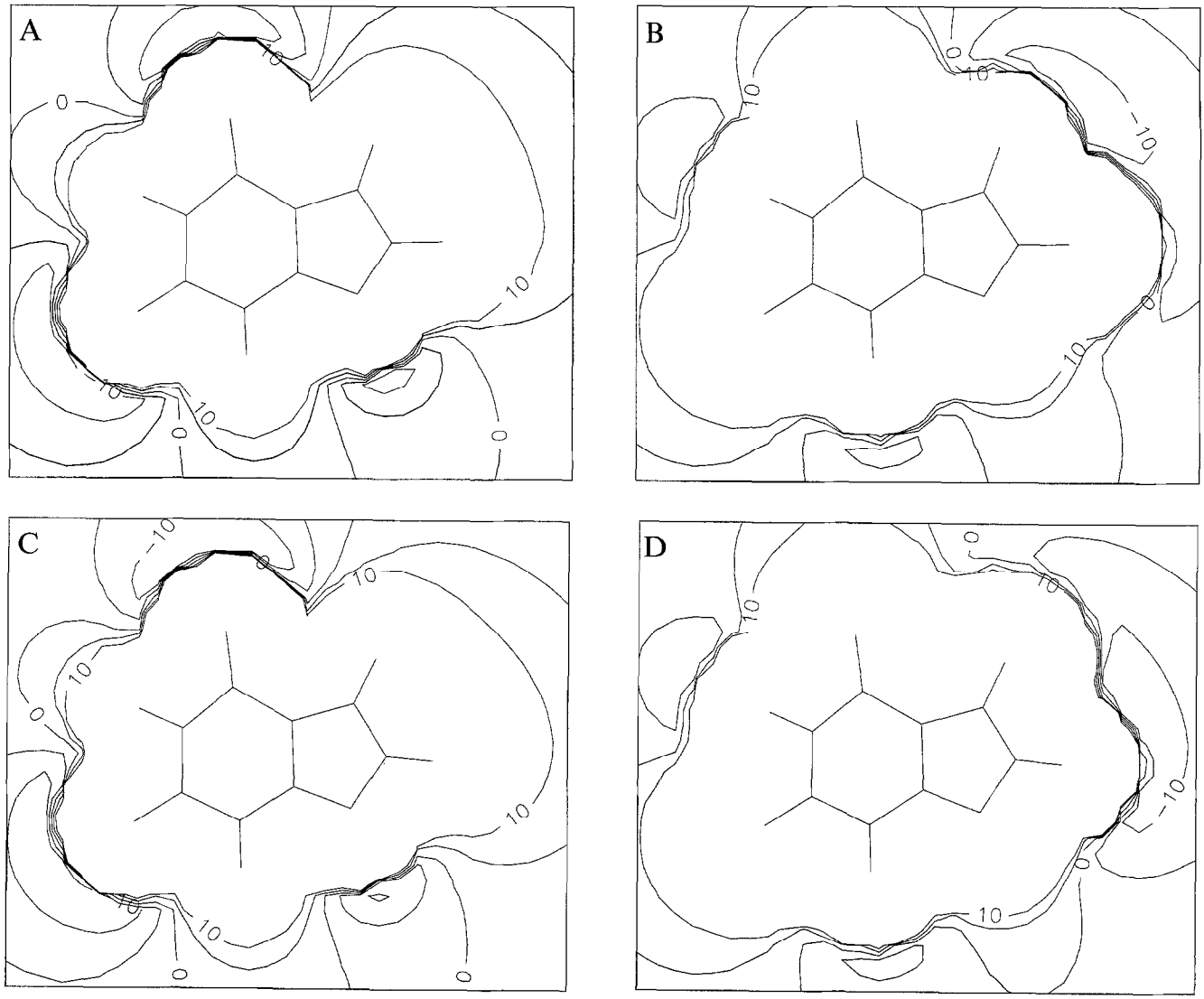

Fig. 5. Maps of molecular interaction potential for the bioactive tautomers of xanthine (X137: A,B) and alloxanthine (Ax138: C,D). The maps correspond to the interaction with hydrogen (A,C) and oxygen (B,D) atoms. Charges of +0.5 and −0.5 were defined for hydrogen and oxygen, respectively.

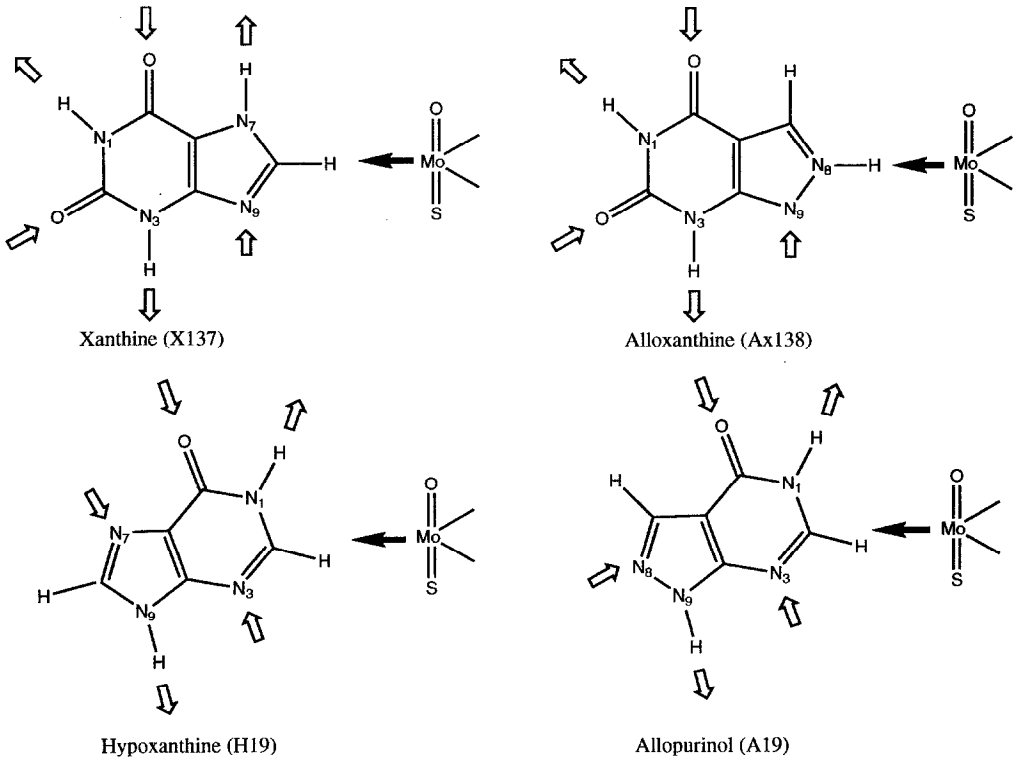

Fig. 6. Scheme of the potential hydrogen-bond interactions for the bioactive tautomers of xanthine (X137), alloxanthine (Ax138), hypoxanthine (H19) and allopurinol (A19).

Inspection of the results in Table 2, which gives the relative stabilities determined in the final ab initio study between the selected tautomers, shows a clear preference for Ax138. Thus, the keto species Ax139 is less favored by 4.8 kcal/mol at the MP2/6-31+G(d,p) level, and such destabilization amounts to 9 kcal/mol or even more for the keto–enol species Ax192t and Ax182t.

Tautomerism of xanthine and alloxanthine in aqueous solution

SCRF calculations were performed to analyze the solvent effect on the tautomerism of xanthine and alloxanthine with a twofold purpose. Firstly, the influence of solvent-induced geometry changes on the relative stability between tautomers was investigated from AM1-SM2 calculations [21]. Secondly, the magnitude of the solvent effect on tautomeric equilibria was examined using two different continuum models: the generalized Born model as implemented in the AM1-SM2 model, and our AM1 and 6-31G(d) optimized versions [17,18] of the Polarizable Continuum Model developed by Tomasi's group [19]. The reliability of the solvent-induced stabilization can be assessed by comparison of the corresponding relative free energies of hydration. The differences in the free energy of hydration ($\Delta\Delta G^{hyd}_{A\to B}$) for selected tautomers of xanthine and alloxanthine are given in Tables 3 and 4.

Inspection of the AM1-SM2 values indicates that the solvent-induced geometrical changes have, in general, a small effect on the relative free energy of hydration. The largest change in the free energy of hydration upon geometry optimization, which amounts to 1.0 kcal/mol, is found for the tautomer Ax139. The root-mean-square deviation in the relative free energies of hydration determined with and without geometry optimization for all the tautomers amounts to 0.5 kcal/mol, which probably lies beyond the accuracy of the calculations [21]. This suggests that changes in structural parameters do not significantly modify the relative free energy of hydration upon solvation of the tautomers, supporting the use of gas-phase geometries in MST calculations.

Comparison of the results determined from AMSOL and MST calculations reveals reasonable agreement for the keto–enol tautomers. The difference between AM1-SM2 and MST relative free energies of hydration for the di-keto forms X139 and Ax139, however, increases to 3 kcal/mol, the MST results indicating a larger stabilization upon solvation than the AM1-SM2 estimates. In spite of the quantitative differences in the free energies of hydration, both AM1-SM2 and MST results indicate that the tautomeric preference in the gas phase is not drastically altered upon transfer to aqueous solution. This is clearly shown by the relative free energies of tautomerization in aqueous solution ($\Delta G^{aq}_{A\to B}$), which are reported in Tables 5 and 6 for tautomers of xanthine and alloxanthine, respectively. Values of $\Delta G^{aq}_{A\to B}$ were determined according to Eq. 1 using the AM1-SM2 and MST free energies of

hydration, while the free energy of tautomerization in the gas phase ($\Delta G^{gas}_{A\rightarrow B}$) was taken from the value computed at the MP2/6-31+G(d,p) level (Tables 1 and 2).

The results in Table 5 indicate that the tautomer X137 of xanthine is the predominant species in aqueous solution. The tautomer X139 is disfavored by at least 3.6 kcal/mol and the keto–enol species (X192t and X172t) are destabilized by more than 8 kcal/mol. For alloxanthine, the tautomer Ax138 is also the most stable form, the di-keto species Ax139 being less favored by at least 3.3 kcal/mol. The difference in stability for the keto–enol tautomers Ax192t and Ax182t is larger than 5.6 kcal/mol.

Discussion

Knowledge of the tautomerism of neutral xanthine and alloxanthine has been gained from high-level QM ab initio calculations and SCRF continuum methods. Since a specific scheme of hydrogen-bond donors and acceptors characterizes each tautomer, inspection of the predominant tautomeric forms can be used to understand their recognition as substrates by the enzyme xanthine oxidase.

Considering the size of the molecules, the level of ab initio calculation (MP2/6-31+G(d,p)) used in this study is large enough to be confident in the quality of the results. However, an additional test of quality of our highest level calculations can be gained from the convergence achieved as the computational level is increased. The reliability of the relative stability between tautomers in the gas phase is supported by the similar results obtained using different levels of theory, especially when a large, flexible basis set is used (Tables 1 and 2). The agreement also extends reasonably well to the values computed at the HF/6-31G(d) level, which gives confidence in the stepwise elimination protocol. Further support also stems from the similarity with the non-local DFT results.

The present results indicate that xanthine exists in the gas phase mainly, if not exclusively, in the form X137, since this tautomer is stabilized by more than 8.8 kcal/mol at the MP2/6-31+G(d,p) level over the di-keto (X139) and keto–enol forms (X192t and X172t). This agrees with previous CNDO [26] and HF/MIDI [27] estimates of the energy difference between species X137 and X139, which predict the latter form to be disfavored (in energy) by 7–8 kcal/mol. Recently, the energy difference (with inclusion of zero-point energy corrections) at the MP2/6-311G-(d,p)//HF/6-31G(d,p) level has been estimated to be 9.1 kcal/mol, with the X137 form being more stable than X139 [28]. In addition, X137 is more stable than the keto–enol species X192t and X172t by 10.1 and 10.9 kcal/mol, respectively [28].

Our best estimates of the relative stability between tautomers of alloxanthine point out that Ax138 is predominant in the gas phase, as noted by the free energy difference of 4.8 kcal/mol obtained with our highest level of calculation (3.5–4.2 kcal/mol from lower level calculations). Previous HF/MIDI calculations [27] estimated the energy difference with respect to the Ax138 tautomer to be about 3 kcal/mol, which is similar to our HF/6-31G(d) value. In summary, all theoretical data indicate that Ax138 is the major species. To our knowledge there are no experimental data available for comparison, but the MP2/6-31+G(d,p) differences in stability are large enough to assure that Ax138 is the main, if not unique, tautomer of alloxanthine in the gas phase.

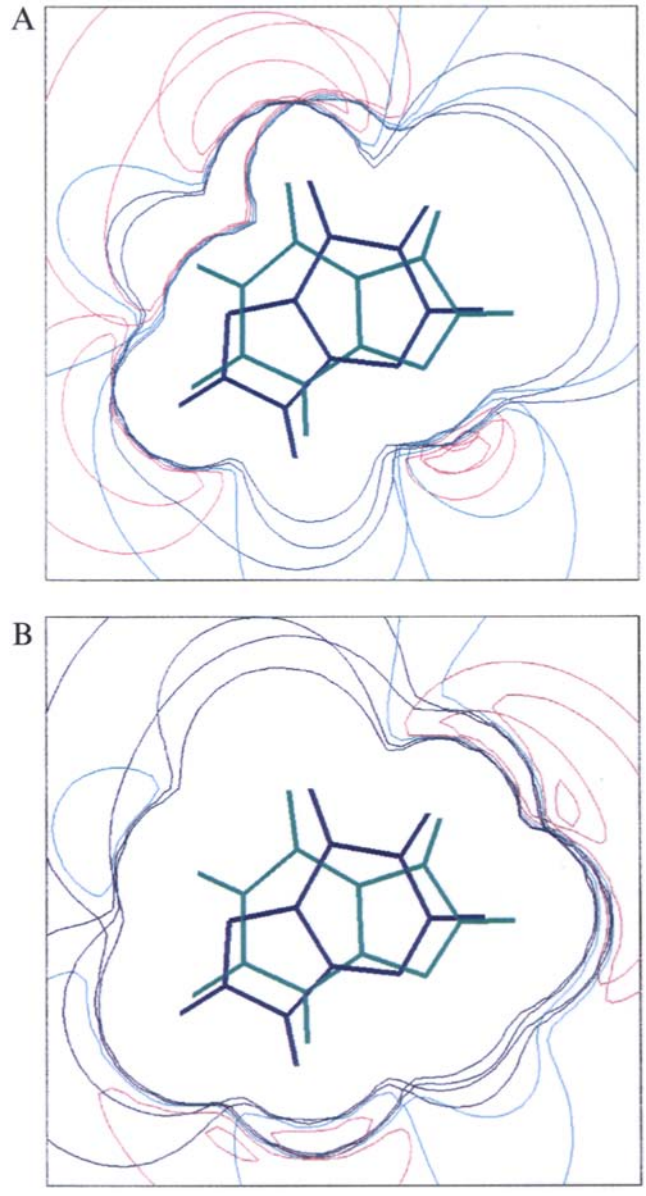

Fig. 7. Superposition of the maps of molecular interaction potential for the tautomers X137 (green) and H19 (blue) of xanthine and hypoxanthine. The maps correspond to the interaction with hydrogen (A) and with oxygen (B) atoms. Charges of +0.5 and –0.5 were defined for hydrogen and oxygen, respectively. Negative, zero and positive isocontour lines are shown in pink, light blue and dark blue, respectively.

AM1-SM2 results indicate that solvent-induced geometry changes have little effect on the relative free energies of hydration, which supports the use of gas-phase geometries in MST calculations. There is a general agreement between AM1-MST and AM1-SM2 calculations, but some differences exist, particularly for the di-keto forms. A similar disagreement was also found in a study of the tautomerism of the related compounds hypoxanthine and allopurinol [9]. This discrepancy can be attributed to the intrinsic parametrization of these continuum models, since MST free energies of solvation determined at the AM1 and ab initio 6-31G(d) levels are very similar. The close similarity between AM1-SM2 and MST (especially at the AM1 level) values is remarkable for the keto–enol tautomerism. Overall, despite numerical differences, both AM1-SM2 and MST results clearly indicate that the solvent-induced stabilization does not alter the gas-phase tautomeric preference of either xanthine or alloxanthine. According to the results in Tables 5 and 6, a negligible population of keto–enol tautomers is expected in water, since they are largely disfavored in aqueous solution, while the di-keto species X139 and Ax139 are destabilized by more than 3 kcal/mol with respect to the most stable tautomers. Therefore, the population of tautomers X137 and Ax138 is expected to be greater than 99%.

SCRF calculations at the HF/6-31G(d,p) level using the Onsager model [29] with geometry optimization for a medium with a dielectric constant of 40 estimated the species X137 of xanthine to be more stable than X139 by 4.2 kcal/mol [28]. This value is close to our estimate of $\Delta G^{aq}_{A\to B}$ determined using MP2/6-31+G(d,p) gas-phase free energies and the MST(6-31G(d)) relative free energy of hydration (4.0 kcal/mol; see Table 5). Comparison of the results with the experimental data shows complete agreement. Both UV and NMR spectra [30] clearly demonstrate that xanthine exists in the lactam form in aqueous solution and that prototropic tautomerism at the imidazole ring favors the N7-H form. Unfortunately, no experimental evidence on tautomerism of alloxanthine in aqueous solution is available, but recent crystallographic data indicate that alloxanthine exists in the N8-H tautomeric form, since coordination to metals occurs through N9 [31].

From the preceding discussion, tautomers X137 and Ax138, which are the predominant species both in the gas phase and in aqueous solution, can be considered to be the 'bioactive' species of xanthine and alloxanthine. The two structures share a similar pattern of hydrogen-bond donors and acceptors, the only difference lying in the relative positions of nitrogens at the five-membered ring. However, this difference is not dramatic in terms of molecular recognition, as shown by the MIP maps corresponding to the interaction energy of X137 and Ax138 with charged hydrogen and oxygen atoms as test probes (see Fig. 5). Inspection of the maps reveals the same distribution of reactive characteristics around the two molecules in front of electrophilic and nucleophilic agents. Particularly, the region surrounding positions 7 and 8 in both xanthine and alloxanthine is clearly susceptible to interaction with a nucleophilic site. Therefore, since substrate recognition is driven by geometrical and electrostatic complementarity with the residues at the binding site, such a pattern of interactions must determine recognition of the bioactive tautomers.

Owing to the close structural similarity between xanthine, alloxanthine, hypoxanthine and allopurinol, all these structures are expected to interact with the same catalytic center upon binding to the enzyme. Comparison of their interaction patterns may help elucidate the basic features modulating substrate recognition. For instance, our previous study on tautomerism of hypoxanthine and allopurinol suggested the keto (N1-H, N9-H) tautomers to be the active species [9]. The pattern of hydrogen-bond sites for all these species is schematically depicted in Fig. 6. In addition, since the oxygen incorporated in the substrate during the reduction process of the enzyme is presumably that of the Mo=O unit, positions 8 of xanthine and 2 of hypoxanthine must occupy the same placement near the molybdenum center. This implies that xanthine (alloxanthine) and hypoxanthine (allopurinol) bind to the catalytic site in a different relative orientation. Accordingly, the comparison of interaction patterns must be performed once the five-membered ring of xanthine and alloxanthine is superimposed onto the pyrimidine ring of hypoxanthine and allopurinol. This can be obtained by a rotation of ~180° around the C4-C5 bond (see below).

Inspection of Fig. 6 suggests that binding of xanthine is mainly driven by a recognition pattern defined by hydrogen-bond donor groups at N3 and N7, and hydrogen-bond acceptor groups at N9 and O6. This interaction pattern is well reproduced by allopurinol and hypoxanthine, since they display hydrogen-bond donor groups at N9 and N1, and hydrogen-bond acceptor groups at N3 and O6. Finally, a very similar pattern is found for alloxanthine, since, as noted before (see Fig. 5), the substitution of the N-H bond by a C-H bond at position 7 does not affect the susceptibility of alloxanthine for recognition of a complementary nucleophilic region at the substrate binding site. According to this recognition pattern, position 2 of xanthine has either none or a negligible effect on substrate binding, since different functional groups (C2=O of xanthine; C8-H in hypoxanthine; N8 in allopurinol) are attached to this or equivalent positions in the bioactive species. Indeed, analogous conclusions can be formulated for the interaction at the N1-H site of xanthine (alloxanthine), since this group is replaced by a pyridine-like nitrogen (N7) in hypoxanthine.

The recognition pattern proposed on the basis of our theoretical results allows an understanding of the experimental evidence available for the enzymatic oxidation of hypoxanthine, xanthine and related structures. Xanthine

oxidase catalyzes the conversion of hypoxanthine (allopurinol) to xanthine (alloxanthine), which is subsequently oxidized to uric acid in humans. According to the recognition model, the product of the first reaction (oxidation at position C2 of hypoxanthine, yielding xanthine) cannot be further oxidized at position 8 in the second reaction, unless it completely changes (around 180°) its orientation inside the binding pocket. However, it is difficult to conceive such a large rearrangement because of the large steric hindrance with groups at the active site. Instead, it seems more reasonable to assume that xanthine leaves the active site before reentering as a substrate for the second oxidative process with the proper alignment to fit the binding pocket. This agrees with the existence of a ping-pong mechanism for this enzyme [32].

Further support to the recognition pattern stems from the fact that all the mono-*N*-methylated derivatives of xanthine*, with the exception of 1-methylxanthine, are not oxidized by the enzyme. Similarly, the *N*-methyl derivatives of hypoxanthine are also refractory or are oxidized at a much slower rate than the parent compound [32]. This can be understood from our results considering that methylation leads to the blockage of essential interactions between the bioactive species with groups at the binding site. The refractoriness of 7-methylhypoxanthine, in which the position of the methyl group is equivalent to that for 1-methylxanthine (see Fig. 6), may be surprising. Nevertheless, in this methyl derivative hypoxanthine can no longer exist as tautomer H19, since no hydrogen atom is attached to N9, and this would impede interaction with a hypothetical hydrogen-bond acceptor at the binding site. Indeed, the fact that 8-methylhypoxanthine has nearly the same rate of oxidation as the parent compound reinforces the conclusion that this position does not modulate recognition by the enzyme.

Do the groups responsible for recognition of xanthine and hypoxanthine lie in the correct geometrical alignment for interaction with the enzyme binding site? When the MIP maps of tautomers X137 of xanthine and H19 of hypoxanthine are superimposed, the distribution of the regions susceptible to attack by electrophilic and nucleophilic agents are perfectly matched (see Fig. 7). This fitting only requires a small rotation (around 20°) of the local reference system of hypoxanthine relative to that used for xanthine, which allows superposition of the groups involved in recognition within the enzyme active site. Similar results are obtained when the MIP maps for xanthine are superimposed with those for alloxanthine and allopurinol in the orientation shown in Fig. 6 (results not shown).

*Data for 7-methylxanthine are controversial, since in Ref. 32a it is found to be refractory to oxidation by xanthine oxidase, but in Ref. 32b it is reported to be oxidized at a rate slower (about 1/10) than that measured for xanthine.

Further implications in the binding of alloxanthine can be envisaged from the recognition model. It has been shown that interaction between a nitrogen atom and the molybdenum occurs upon binding [3c]. Several structural models for coordination of alloxanthine to the molybdenum have been proposed to explain this finding. In these models alloxanthine is ligated through N8 [3c,d], N9 [33], or even via bidentate coordination through N8 and N9 [34]. Our results suggest that alloxanthine follows the same pattern as xanthine, so that N9 is recognized by a hydrogen-bond donor group of the enzyme, while the molybdenum is located near N8 (C8 in xanthine). Accordingly, a plausible model for the inhibitory complex is the binding of the molybdenum to N8 of alloxanthine after loss of the proton attached to N8. At this point, it is worth noting that experimental data suggest that oxidation of xanthine is initiated by abstraction of the acidic proton bound to position 8, followed by carbanion attack on the Mo=O unit [4d,35]. Such an initiation reaction is expected to be more favorable for alloxanthine, where a nitrogen replaces the carbon at position 8. This justifies the experimentally determined data for binding of alloxanthine [4d], which reveal fast formation of the reversible complex with the reduced enzyme. Note that this fast process should be followed by a slower step in which alloxanthine coordinates to the molybdenum displacing an oxygen ligand of the metal, leading to enzyme inhibition [4d].

Conclusions

Tautomerism of xanthine and alloxanthine shows a clear preference for the di-keto tautomers both in the gas phase and in aqueous solution. The prototropic tautomerism at the imidazole and pyrazole rings clearly favors the N7-H and N8-H forms of xanthine and alloxanthine, respectively. These tautomers can be considered as the bioactive species in the binding to the enzyme xanthine oxidase.

Comparison of the reactivity patterns for the bioactive tautomers of xanthine and alloxanthine with those for the bioactive species of hypoxanthine and allopurinol allows to define the basic features of the recognition by xanthine oxidase. Two types of interaction appear to be responsible for substrate recognition, corresponding to interaction of hydrogen-bond donors with N3 and N7 and hydrogen-bond acceptors with N9 and O6 in the case of xanthine. This recognition pattern, which can be extended to the binding of hypoxanthine, allopurinol and alloxanthine, allows to explain experimental data available on the enzymatic mechanism of xanthine oxidase. Extension of present studies to the tautomerism of other purine-like substrates may provide an additional basis to test the suitability of this scheme of interactions, which may be valuable for the design of new specific inhibitors.

Acknowledgements

We thank Prof. J.Tomasi for a copy of the MST routines, which were modified by us to perform the present study. We also thank Prof. G. Shields and Prof. R. Poupplana for his critical comments. This work was supported by the Centre de Supercomputació de Catalunya (CESCA, Mol. Recog. Project) and the Dirección General de Investigación Científica y Técnica (PB93-0779 and PB94-0940).

References

1 a. Dixon, M., Biochem. J., 20 (1926) 703.
b. Booth, V.H., Biochem. J., 32 (1938) 494.
2 Rundles, R.W., Wyngaarden, J.B., Hitchings, G.H., Elion, G.B. and Silberman, H.P., Trans. Assoc. Am. Phys., 76 (1963) 126.
3 a. Hille, R. and Massey, V., Pharmacol. Ther., 14 (1981) 249.
b. Hille, R. and Massey, V., J. Biol. Chem., 256 (1981) 9090.
c. Hawkes, T.R., George, G.N. and Bray, R.C., Biochem. J., 218 (1984) 961.
d. Hille, R., George, G.N., Eidsness, M.K. and Cramer, S.P., Inorg. Chem., 28 (1989) 4018.
4 a. Bray, R.C., In Boyer, P.D. (Ed.) The Enzymes, Vol. 12, Academic Press, New York, NY, U.S.A., 1975, p. 299.
b. Coughlan, M.P., Johnson, J.L. and Rajagopalan, K.V., J. Biol. Chem., 255 (1980) 2694.
c. Hille, R. and Massey, V., In Spiro, T.G. (Ed.) Molybdenum Enzymes, Wiley, New York, NY, U.S.A., 1985, p. 443.
d. Hille, R., Biochim. Biophys. Acta, 1184 (1994) 143.
5 Rajagopalan, K.V., Adv. Enzymol., 64 (1991) 215.
6 Coughlan, M.P. and Rajagopalan, K.V., Eur. J. Biochem., 105 (1980) 81.
7 Skibo, E.B., Biochemistry, 25 (1986) 4189.
8 a. McCollister, R.J., Gilbert Jr., W.R., Ashton, D.M. and Wyngaarden, J.B., J. Biol. Chem., 239 (1964) 1560.
b. Krenitsky, T.A., Elion, G.B., Strelitz, R.A. and Hitchings, G.H., J. Biol. Chem., 242 (1967) 2675.
c. Chalmers, R.E., Parker, R., Simmonds, H.A., Snedden, W. and Watts, R.W.E., Biochem. J., 112 (1969) 527.
9 Hernández, B., Luque, F.J. and Orozco, M., J. Org. Chem., 61 (1996) 5964.
10 Dewar, M.J.S., Zoebisch, E.G., Healy, E.F. and Stewart, J.J.P., J. Am. Chem. Soc., 107 (1985) 3902.
11 Hariharan, P.C. and Pople, J.A., Theor. Chim. Acta, 28 (1973) 213.
12 Møller, C. and Plesset, M.S., Phys. Rev., 46 (1934) 618.
13 Frisch, M.J., Pople, J.A. and Binkley, J.S., J. Chem. Phys., 80 (1984) 3265.
14 a. Becke, A.D., J. Chem. Phys., 98 (1993) 5648.
b. Lee, C., Yang, W. and Parr, R.G., Phys. Rev., B37 (1988) 785.
15 Colominas, C., Luque, F.J. and Orozco, M., J. Am. Chem. Soc., 118 (1996) 6811.
16 Frisch, M.J., Trucks, G.W., Head-Gordon, M., Gill, P.M.W., Wong, M.W., Foresman, J.B., Johnson, B.G., Schlegel, H.B., Robb, M.A., Replogle, E.S., Gomperts, R., Andres, J.L., Raghavachari, K., Binkley, J.S., Gonzalez, C., Martin, R.L., Fox, D.J., Defrees, D.J., Baker, J., Stewart, J.J.P. and Pople, J.A., GAUSSIAN '92, Gaussian Inc., Pittsburgh, PA, U.S.A., 1992.
17 a. Luque, F.J., Bachs, M. and Orozco, M., J. Comput. Chem., 15 (1994) 847.
b. Orozco, M., Bachs, M. and Luque, F.J., J. Comput. Chem., 16 (1995) 563.
18 Bachs, M., Luque, F.J. and Orozco, M., J. Comput. Chem., 15 (1994) 446.
19 a. Miertus, S., Scrocco, E. and Tomasi, J., Chem. Phys., 55 (1981) 117.
b. Miertus, S. and Tomasi, J., Chem. Phys., 65 (1982) 239.
c. Tomasi, J. and Persico, M., Chem. Rev., 94 (1994) 2027.
20 a. Orozco, M. and Luque, F.J., J. Am. Chem. Soc., 117 (1995) 1378.
b. Luque, F.J., Cossi, M. and Tomasi, J., J. Mol. Struct. (THEOCHEM), in press.
21 a. Cramer, C.J. and Truhlar, D.G., Science, 256 (1992) 213.
b. Cramer, C.J. and Truhlar, D.G., J. Comput.-Aided Mol. Design, 6 (1992) 629.
22 a. Orozco, M. and Luque, F.J., J. Comput. Chem., 14 (1993) 587.
b. Alhambra, C., Luque, F.J. and Orozco, M., J. Phys. Chem., 99 (1995) 3084.
c. Luque, F.J. and Orozco, M., MOPETE/MOPFIT Computer Program, University of Barcelona, Barcelona, Spain, 1995.
23 Stewart, J.J.P., MOPAC93, Rev. 2, Fujitsu Ltd., 1993.
24 Peterson, M. and Poirier, R., MONSTERGAUSS, University of Toronto, Toronto, ON, Canada, version modified by Cammi, R., Bonaccorsi, R. and Tomasi, J., 1987, and by Luque, F.J. and Orozco, M., 1994.
25 Cramer, C.J., Lynh, G.C. and Truhlar, D.G., AMSOL v. 3.0, based on AMPAC v. 2.1, by Liotard, D.A., Healy, E.F. and Dewar, M.J.S., University of Minnesota, Minneapolis, MN, U.S.A., 1992.
26 Pullman, B., In Bergmann, E.D. (Ed.) Jerusalem Symposia on Quantum Chemistry and Biochemistry, Vol. 2, Jerusalem, Israel, 1970, p. 292.
27 Nonella, M., Hänggi, G. and Dubler, E., J. Mol. Struct. (THEOCHEM), 279 (1993) 173.
28 Sponer, J. and Leszczynski, J., Struct. Chem., 6 (1995) 281.
29 Wong, M.W., Frisch, M.J. and Wiberg, K.B., J. Am. Chem. Soc., 113 (1991) 4776.
30 Lichtenberg, D., Bergmann, F. and Neiman, Z., J. Chem. Soc., C (1971) 1676.
31 a. Hänggi, G., Schmalle, H. and Dubler, E., Inorg. Chem., 32 (1993) 6095.
b. Hänggi, G., Schmalle, H. and Dubler, E., Acta Crystallogr., C50 (1994) 388.
32 a. Bergmann, F., Kwietny, H., Levin, G. and Brown, D.J., J. Am. Chem. Soc., 82 (1960) 598.
b. Bergmann, F. and Levene, L., Biochim. Biophys. Acta, 429 (1976) 672.
33 Stiefel, E.I., Prog. Inorg. Chem., 22 (1977) 1.
34 Robins, K., Revankar, G.R., O'Brien, D.E., Springer, R.H., Novinson, T., Albert, A., Senga, K., Miller, J.P. and Streeter, D.G., J. Heterocycl. Chem., 22 (1985) 601.
35 McWhirther, R.B. and Hille, R., J. Biol. Chem., 266 (1991) 23724.